PAPER

NJC
www.rsc.org/njc

X-Ray and neutron powder diffraction studies of the crystal structure of vitamin K_3†

Harriott Nowell and J. Paul Attfield*

Department of Chemistry, University of Cambridge, Lensfield Road, Cambridge, UK CB2 1EW

***Received* (in Cambridge, UK) 29th May 2003, Accepted 9th December 2003**
First published as an Advance Article on the web 12th February 2004

The previously unknown structure of vitamin K_3 (menadione, 2-methyl-1,4-naphthoquinone, $C_{11}H_8O_2$), a synthetic compound from which it is possible to derive the naturally occurring K vitamins, has been solved from X-ray powder diffraction data. Solution was achieved using simulated annealing and restrained Rietveld refinement, using restraints derived from similar known structures. Further refinement has been carried out using neutron diffraction data; this confirmed the molecular packing and allowed further insight into the structural detail with regard to methyl group orientation, thus allowing the proposal of an extensive C–H···O hydrogen bonding scheme by reference to comparable known structures. The crystal structure consists of chains of molecules lying head-to-tail. This study may aid the understanding of the biological activity of vitamin K.

1. Introduction

Vitamin K is required for the maintenance of normal blood coagulation.[1] Vitamin K_3 (menadione, 2-methyl-1,4-naphthoquinone, $C_{11}H_8O_2$), Fig. 1, is a synthetic compound, from which it is possible to derive vitamin K_1 (Fig. 2a) which is naturally occurring in plants such as cabbage and spinach and vitamin K_2 (Fig. 2b) which is synthesised by intestinal organisms.[1,2] There has recently been interest in the possibility of using menadione as an anti-cancer agent.[3] It can be synthesised by oxidation of 2-methylnaphthalene using H_2O_2 and catalytic quantities of CH_3ReO_3.[4] Despite this interest in menadione, its crystal structure has not been determined. We report here the structure determination using powder X-ray and neutron diffraction.

Initial attempts to determine the unit cell of menadione using laboratory powder X-ray diffraction data were unsuccessful because of insufficient resolution and considerable peak overlap in the low angle region of the data. High resolution synchrotron X-ray data have subsequently been used to successfully index the reflections and the crystal structure has been determined *ab initio* using a direct space method. Recent advances in structure solution from powder diffraction data[5] can be partially attributed to the development, over the past decade, of direct space approaches. These involve a search to optimise a trial structure in direct space in order to produce the best possible agreement between experimental and calculated powder diffraction data. Simulated annealing[6] (SA) is often used to implement the global search and has been used here within the DASH[7,8] software. SA is a search method that allows controlled "uphill" steps (*i.e.* steps that worsen the agreement between observed and calculated data) as well as "downhill" steps; this allows escape from local minima and thereby increases the chances of finding the global minimum. Recent examples of the SA approach to crystal structure determination from powder diffraction data are given in refs. 9 to 11.

The best crystal structure model of vitamin K_3 taken from a series of global optimisation attempts is used here as the starting model for restrained Rietveld[12,13] refinement. This is commonly the final step in *ab initio* crystal structure solution from powder diffraction data during which small improvements are made to the structural model. The restraints supplement the observed data effectively increasing the data to parameter ratio. Recently, restrained Rietveld refinement of a 1261 atom protein has been reported.[14]

Despite the high background caused by incoherent scattering from hydrogenous samples, the low hydrogen to non-hydrogen atom ratio for this aromatic molecule raised the possibility of using neutron diffraction data, to improve the characterisation of this light-atom molecular structure. There

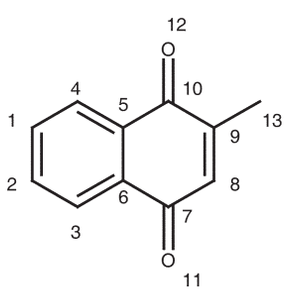

Fig. 1 Non-hydrogen atom numbering in vitamin K_3.

† Electronic supplementary information (ESI) available: X-ray powder diffraction data. See http://www.rsc.org/suppdata/nj/b3/b306072a/

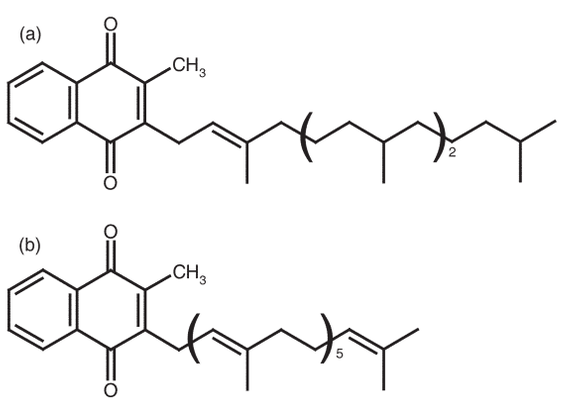

Fig. 2 The molecular structures of (a) vitamin K_1 and (b) vitamin K_2.

DOI: 10.1039/b306072a

are a number of examples where neutron diffraction data have been used for detailed structural studies of organic molecules including *ab initio* crystal structure solutions.[15,16] Restrained Rietveld refinement using the neutron data has confirmed the packing pattern determined using X-ray data and improved the definition of the methyl group orientation allowing an improved proposal of the C–H···O[17] hydrogen bonding scheme in vitamin K_3 by consideration of comparable structures in the Cambridge Structural Database[18] (CSD).

2. Results and discussion

2.1. Data collection

A yellow powdered sample of vitamin K_3 was obtained from Sigma Aldrich. X-Ray diffraction data were collected on BM16 at the European Radiation Synchrotron Facility. The sample was rotated in a 0.8 mm diameter glass capillary. Data collection times were doubled in the second half of the 2θ range to optimise structural information in the pattern.

Time-of-flight neutron diffraction data were collected on the High Resolution Powder Diffractometer[19] (HRPD) at the ISIS spallation source. The sample was held in a vanadium can during data collection and data were collected using detector banks at 168°, 90° and 30°.

2.2. Structure solution using X-ray data

Indexing was carried out using peak positions read from the synchrotron X-ray diffraction profile. This returned a monoclinic cell with lattice parameters $a = 11.1280(10)$Å, $b = 20.6633(24)$Å, $c = 7.4476(5)$Å and $\beta = 97.983(9)°$ and volume = 1695.9Å^3 with high figures of merit ($M(23) = 54.5$ and $F(23) = 370.2$). Previous attempts to index the data collected on a laboratory instrument were unsuccessful because of an unobserved weak $\bar{2}31$ reflection (at $2\theta = 8.79°$) in the BM16 data and overlapping 022, $\bar{3}20$ and $\bar{1}22$ reflections at $2\theta = 9.89$, 9.92 and 9.97° respectively (the laboratory data, $\lambda = 1.54056$ Å, have been provided as ESI†). This illustrates the importance of high peak to background ratio for indexing such complex cells. A Pawley fit[20] using space group $P2_1/a$, resulted in $\chi^2_{\text{Pawley}} = 8.7$. Comparison of molecular volume and unit cell volume indicated the presence of two molecules in the asymmetric unit. A number of simulated annealing (SA) runs (>30) were carried out, using intensity information taken from this Pawley fit. The position and orientation of the rigid molecular fragment (a total of six degrees of freedom) were optimised during SA. A physically reasonable crystal structure, with $\chi^2 = 44.64$, was chosen for further investigation using Rietveld refinement. A number of the global optimisation attempts produced similar results and others ended with physically unreasonable crystal structures.

2.3. Restrained Rietveld refinement using X-ray data

All bond lengths and angles were restrained during refinement, each restraint consisting of an ideal value, r_i, and an associated standard uncertainty, σ. Based on a method introduced previously[21–23] the bond length restraints were defined using the mean and standard deviation of a sample of comparable bond lengths from known structures as r_i and σ respectively. Structures containing appropriate fragments of the target molecule, shown in Fig. 3, were found in the Cambridge Structural Database (CSD), using the Conquest search algorithm[24] and used as the sample of comparable bond lengths. Table 1 lists the bond length restraints determined from each search, r_i and σ for each restraint are given in Table 2. Unfortunately, the sample used to define C_{aromatic}–C_{aromatic} bond length restraints (search 1) is rather small; only ideal values were derived from this search and all standard uncertainties for these bonds were set to 0.02 Å. Bond angles in the aromatic system were restrained using $r_i = 120°$ and $\sigma = 2°$, angles in the methyl group were restrained using $r_i = 109°$ and $\sigma = 7°$. Both molecules (A and B) in the asymmetric unit were restrained using identical values. Atoms in and adjacent to the ring system were restrained ($\sigma = 0.01$ Å) to lie in the same plane.

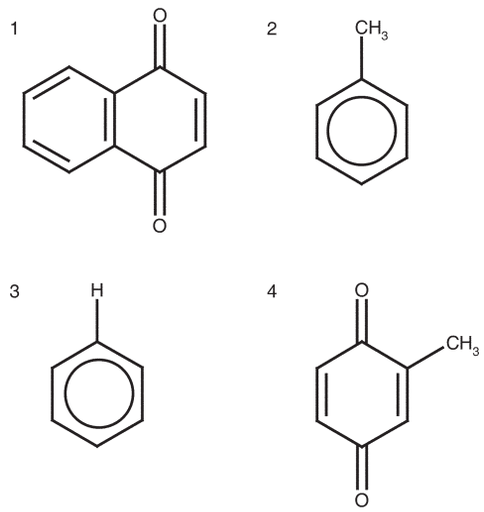

Fig. 3 Search fragments used to search the CSD for known structures from which define bond length restraints for vitamin K_3. Searches for fragments 2 and 3 included neutron studies only.

A twelve term linear interpolation background function, peak shapes, lattice parameters, zero point and scale factor were refined initially. The peak width variation with 2θ was modelled using $(X + X_e\cos\phi)/\cos\theta$ to allow for anisotropic particle size broadening. ϕ is the angle between the *hkl* plane normal and the [001] axis and X and X_e are refined coefficients.[25] An asymmetry correction was also applied.[26] All atom positions were refined subject to the restraints described above. Preferred orientation was refined along the [001] axis using the March Dollase function,[27,28] the ratio converged to a value <1, indicating the presence of needle shaped crystallites. Further refinement details are given in Table 3. An acceptable profile fit was obtained, shown in Fig. 4, with $\chi^2 = 8.79$ and $R_F^2 = 0.1076$. χ^2 is considerably lower for the profile fit of the final refined model than for the structural model at the end of the simulated annealing run; this may be partially attributed to improved peak shape description, modelling of preferred orientation and small changes to temperature factors and molecular geometry. Refined bond lengths are given in Table 2 and refined angles and their restraints have been provided as supplementary information.†

3.4. Restrained Rietveld refinement using neutron data

Structure refinement using neutron diffraction data confirmed that the proposed crystal structure was sensible. A procedure

Table 1 Search fragment details (search numbers correspond to fragments in Fig. 3)

Search	Search restrictions	Number of fragments	Bond length restraints defined
1	None	10 structures (14 fragments)	C_{aromatic}–C_{aromatic}
2	Neutron studies only	21 structures (61 fragments)	C_{methyl}–H
3	Neutron studies only	201 structures (2148 fragments)	C_{aromatic}–H
4	None	50 structures (81 fragments)	C=O C_{aromatic}–C_{methyl}

Table 2 Bond length restraints; atomic numbering is shown in Fig. 1, A and B denote the two molecules in the asymmetric unit

			X-Ray				Neutron			
	Restraint values		A		B		A		B	
Bond	r_i/Å	σ/Å	r_c/Å	$(r_i - r_c)^2/\sigma^2$	r_c/Å	$(r_i - r_c)^2/\sigma^2$	r_c/Å	$(r_i - r_c)^2/\sigma^2$	r_c/Å	$(r_i - r_c)^2/\sigma^2$
C1–C2	1.40	0.02	1.387(5)	0.42	1.407(5)	0.12	1.406(1)	0.09	1.401(1)	0.00
C2–C3	1.39	0.02	1.398(5)	0.16	1.399(5)	0.20	1.388(1)	0.01	1.388(1)	0.01
C3–C6	1.40	0.02	1.392(5)	0.16	1.384(5)	0.64	1.400(1)	0.00	1.394(1)	0.09
C6–C5	1.41	0.02	1.401(5)	0.20	1.414(5)	0.04	1.405(1)	0.06	1.410(1)	0.00
C5–C4	1.40	0.02	1.398(5)	0.01	1.385(5)	0.56	1.401(1)	0.00	1.396(1)	0.04
C4–C1	1.39	0.02	1.389(5)	0.00	1.374(5)	0.64	1.389(1)	0.00	1.393(1)	0.02
C6–C7	1.47	0.02	1.467(5)	0.02	1.471(5)	0.00	1.468(1)	0.01	1.465(1)	0.06
C5–C10	1.48	0.02	1.479(5)	0.00	1.469(5)	0.30	1.483(1)	0.02	1.479(1)	0.00
C9–C8	1.38	0.02	1.366(5)	0.49	1.383(5)	0.02	1.380(1)	0.00	1.380(1)	0.00
C9–C10	1.47	0.02	1.453(5)	0.72	1.469(5)	0.00	1.471(1)	0.00	1.470(1)	0.00
C7–C8	1.50	0.02	1.484(5)	0.64	1.502(5)	0.01	1.498(1)	0.01	1.496(1)	0.04
C7–O11	1.23	0.02	1.231(5)	0.00	1.238(5)	0.16	1.228(1)	0.01	1.230(1)	0.00
C10–O12	1.23	0.01	1.229(3)	0.01	1.234(3)	0.16	1.2287(7)	0.02	1.2306(7)	0.00
C9–C13	1.50	0.02	1.491(5)	0.20	1.488(5)	0.36	1.499(1)	0.00	1.496(1)	0.04
C4–H17	1.08	0.03	1.085(9)	0.03	1.082(9)	0.00	1.078(2)	0.00	1.079(2)	0.00
C1–H14	1.08	0.03	1.082(9)	0.00	1.085(9)	0.03	1.084(2)	0.02	1.078(2)	0.00
C2–H15	1.08	0.03	1.074(9)	0.04	1.084(9)	0.02	1.076(2)	0.02	1.083(2)	0.01
C3–H16	1.08	0.03	1.080(9)	0.00	1.079(9)	0.00	1.081(2)	0.00	1.077(2)	0.01
C8–H18	1.08	0.03	1.081(9)	0.00	1.079(9)	0.00	1.081(2)	0.00	1.077(2)	0.01
C13–H19	1.07	0.03	1.071(9)	0.00	1.075(9)	0.03	1.068(2)	0.00	1.069(2)	0.00
C13–H20	1.07	0.03	1.072(9)	0.00	1.073(9)	0.01	1.072(2)	0.00	1.064(2)	0.04
C13–H21	1.07	0.03	1.072(9)	0.00	1.069(9)	0.00	1.069(2)	0.00	1.069(2)	0.00

similar to that used for the X-ray refinement was followed and the same bond length, angle and planar group restraints were used. Data from all three detector banks were fitted simultaneously to maximise the information available. Backgrounds were modelled using twelve term linear interpolation functions. Peak shapes were described using a convolution of Gaussian ($\sigma^2 = G^2d^2$) and Lorentzian ($\gamma = Ld$) peak width variations with d-spacing, d, where G and L are refined parameters. Lattice parameters and zero point were refined before allowing the atom positions to refine.

There are two main differences between the refinements using X-ray and neutron data. Firstly, hydrogen atom temperature factors were refined using the neutron data but this was not possible with the X-ray data. Secondly, preferred orientation of the sample was not included during refinement using neutron data as no convincing evidence of its presence was found. Anisotropic refinement of the oxygen atoms was attempted with neutron data but led to non-positive definite thermal ellipsoids and was therefore not pursued. Excellent fits to all three data sets were obtained, with a combined goodness of fit of $\chi^2 = 7.42$. The fit to the 90° detector data is shown in Fig. 5.

2.5. Strength of restraints used during refinement

To ensure stability during initial cycles of refinement, strong restraints were initially imposed, but these were relaxed during the course of refinement and the global weight factor for the restraints, f, was reduced to the lowest value at which $(r_i - r_c)^2/\sigma^2 \leq 1$ for all bond lengths and angles. This criterion was used for both refinements and has been used previously.[22] In the refinement using the X-ray data, f was reduced to 100, giving a 2.5% contribution to χ^2 from the restraints. In the analysis of the neutron data f was reduced to 1700, a 2.3% contribution to χ^2 from the restraints. See Table 2 for values of $(r_i - r_c)^2/\sigma^2$ for bond lengths, from both refinements. Values of $(r_i - r_c)^2/\sigma^2$ for angles have been provided as supplementary information.† Thus, the contribution from the restraints is very low in both cases, ensuring the diffraction data (rather than the restraints) have the greater influence on the final structure. Note that the value of f in the final cycle of the neutron refinement is seventeen times larger than for the X-ray refinement, however the contribution to χ^2 from the restraints makes up approximately the same proportion of the total. The influence of the restraints therefore does not appear to be much greater in this refinement; it is enough, however, to compensate for the loss of structural information in the neutron data because of high incoherent background scattering from this hydrogenous sample, and produce a crystal structure of similar quality to the X-ray model.

2.6. Comparison of structures determined from X-ray and neutron diffraction data

Clearly, the use of the same ideal distances and angles in the restrained X-ray and neutron refinements imposes a high degree of similarity between the crystal structures. However there are no restraints imposed on the translation or rotation of the molecular unit, or on the characteristics of any intermolecular interactions and it is therefore possible for the structures to differ quite considerably in these respects.

There is good agreement between the crystal structures obtained from the two refinements. An overlay of the two molecules in the asymmetric units of the two structures is shown in Fig. 6. The largest disagreement between the two structures is the position of the hydrogen atoms in the methyl groups caused by a rotation of ~50° about the $C_{aromatic}$–C_{methyl} bond. The resulting disagreements in hydrogen atom positions range between 0.785 Å and 0.906 Å. Since the hydrogen atoms are very poorly represented in X-ray diffraction data this disagreement is not unexpected and the positions deduced from the neutron refinement are considered the more accurate. The hydrogen bonding description is therefore improved through the use of neutron data and will be discussed further in the following section. Agreement between the two structures with regard to the positions of all other equivalent atoms is good; all atoms have a displacement of <0.1 Å with the exception of O32 (with a displacement of 0.13 Å). Residuals and

Table 3 Refinement details

	X-Ray	Neutron
Data collection	1 to 28° (2θ) Step size 0.003° (2θ) λ = 0.598542(3) Å	Time of flight 50–150 ms
Number of *hkl* reflections	937	931
Observations		
Profile points	9000	28 396
Bond length restraints	44	44
Bond angle restraints	72	72
Observations involved in planar group restraints	50	50
Total observations	9166	28 557
Parameters		
Profile	22	47
Atom	128	114
Total parameters	150	161
Global weight factor on restraints	100	1700
Space group	$P2_1/a$	
Z	8	
Z'	2	
Lattice parameters		
a/Å	11.1325(1)	11.1110(3)
b/Å	20.6726(2)	20.6416(5)
c/Å	7.44834(5)	7.4343(1)
β/°	97.985(1)	97.949(1)
Unit cell volume/Å^3	1697.52(3)	1688.66(8)
U_{iso}/Å^2		
C	0.070(1)	0.0161(5)
O	0.095(2)	0.037(2)
H_{methyl}	0.025 (Not refined)	0.074(3)
$H_{non\text{-}methyl}$	0.025 (Not refined)	0.069(2)
Preferred orientation		
Axis	001	Not refined
Ratio	0.905(1)	
Residuals		
R_{wp}	0.0906	0.0123
R_p	0.0714	0.033
χ^2		
Profile contribution to χ^2	77 251	2 05 547
Restraints contribution χ^2	2000	4926.5
Total χ^2	79 251	210473.5
Reduced χ^2	8.790	7.416

standard uncertainties are of the same order of magnitude in both refinements.

The lattice parameters calculated in the two refinements are different; all cell lengths calculated from the neutron data are smaller than those calculated from the X-ray data. The largest discrepancy is for b and all have a discrepancy of <0.03 Å. This disagreement can be partially attributed to the scaling of the time of flight neutron data to absolute wavelength.

Crystal Data: $C_{11}H_8O_2$, M = 172.18, monoclinic, space group $P2_1/a$ (no. 14), T = 298 K, Z = 8. X-Ray data were collected in the range 1 to 28° (2θ), step size 0.003° (2θ) using λ = 0.598542(3) Å over a period of ~7 hours. Neutron data were collected using a counting time of ~10 hours. Indexing was carried out in DICVOL91[29] within the Crysfire[30] suite, Pawley fitting and global optimisation of the crystal structure were carried out in DASH[7,8] and Rietveld refinement in GSAS[31] with 166 restraining observations. Refinement using X-ray data: a = 11.1325(1) Å, b = 20.6726(2) Å, c = 7.44834(5) Å, β = 97.985(1)°, volume = 1697.52(3) Å^3, an isotropic temperature factor was refined for carbon and another for oxygen, R_{wp} = 0.0906 and R_p = 0.0714, 9000 data points, 937 reflections, 150 parameters. Refinement using neutron data: a = 11.1110(3) Å, b = 20.6416(5) Å, c = 7.4343(1) Å, β = 97.949(1)°, volume = 1688.66(3)Å^3, four isotropic temperature factors were refined, one for carbon, one for oxygen, one for methyl-hydrogen and another for non-methyl hydrogen, R_{wp} = 0.0123 and R_p = 0.033, 28 396 data points, 931 reflections, 161 parameters. CCDC reference numbers 229590 and 229591. See http://www.rsc.org/suppdata/nj/b3/b306072a/ for crystallographic data in .cif or other electronic format.

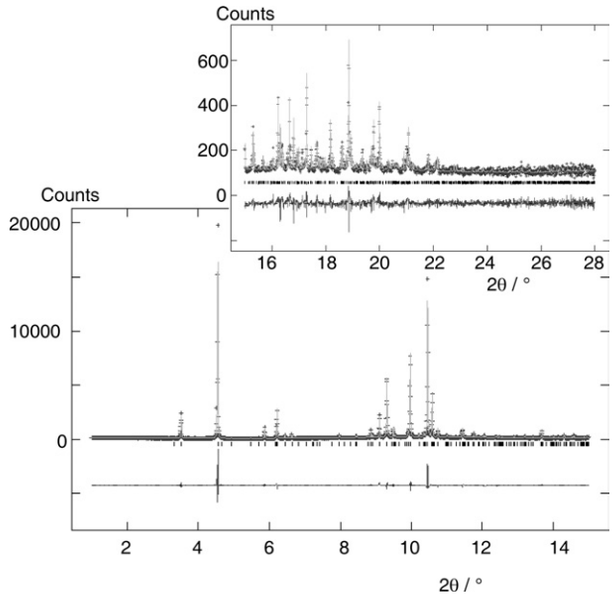

Fig. 4 The final fit between observed synchrotron (dark grey crosses) and calculated (light grey lines) diffraction profiles; the inset shows the high angle region in more detail. The difference plots are also shown.

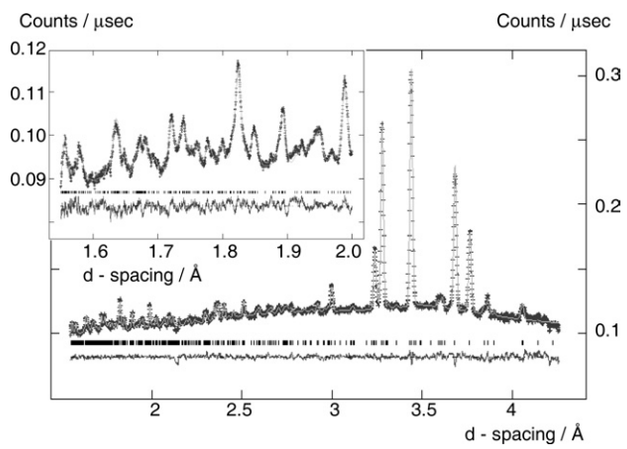

Fig. 5 Agreement between observed neutron (dark grey crosses) and calculated (light grey lines) diffraction profiles for the 90° detector data; the inset shows the low d-space range in more detail. Difference plots are also shown.

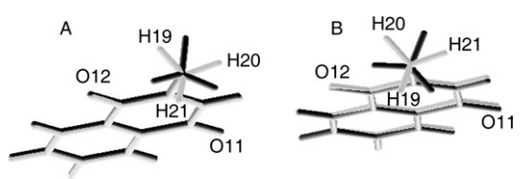

Fig. 6 A comparison of the asymmetric unit determined from X-ray data (dark grey) and neutron data (light grey) with oxygen and methyl-hydrogen atom labels.

2.7. The crystal structure

There are two non-symmetry equivalent molecules (A and B) in the structure of vitamin K_3. Chains consisting of type A molecules lie head-to-tail, antiparallel to chains consisting of type B molecules also lying head-to-tail, but displaced in the direction normal to the plane of the ring, see Fig. 7. C–H···O hydrogen bonds[17] are apparent between neighbouring chains forming sheets parallel to the ring planes. The sheets stack so that the alternating pattern of symmetry equivalent chains continues in the direction normal to the plane of the sheet.

The discrepancy between methyl group hydrogen atoms in the two refinements means that different conclusions were drawn regarding hydrogen bonding once the neutron data had been fitted and the structure refined using the neutron data is used for the following discussion.

From consideration of structures in the CSD, it is more common for the oxygen atom in such a system to be involved in two hydrogen bonding interactions rather than just one single linear hydrogen bond. This can be explained because of the attraction of neighbouring hydrogen atoms to the lone pairs of electrons on the oxygen atom. However the two hydrogen bonds are rarely equivalent. It is not uncommon for one hydrogen atom to be considerably further from the oxygen atom than the other, indicating that one hydrogen bond is stronger than the other.

Two intermolecular C–H···O hydrogen bonds can be attributed to each of the four oxygen atoms in the structure described here, leading to eight non-equivalent hydrogen bonding interactions in the asymmetric unit. The hydrogen bonding scheme is proposed in Table 4 and is shown in Fig. 8, the interactions are labelled 1 to 8 and assigned a graph set descriptor.[32,33] Interactions 1, 2, 4, 6 and 7 are simple dimer motifs and 3 is a chain motif parallel to *a* with a repeat unit of five atoms. The remaining two interactions, 5 and 8, are ring motifs both involving two molecules and two interactions per ring (both interactions shown in Fig. 8). Table 4 includes a comparison to 235 similar systems in the CSD, located during a search for the fragment shown in Fig. 9. There were more than two possible hydrogen donors for O12 and O32 so the geometry of similar systems taken from the CSD was used to reduce the ambiguity; particular attention was paid to the C–H···O, C=O···H and H···O···H angles. The crystal structure of vitamin K_3 demonstrates that the menadione molecule can act as both an H-bond acceptor and donor. This structural characteristic may be relevant to the biological activity of vitamin K in, for example, its role in the blood coagulation process during which vitamin K dependent carboxylase converts glutamyl residues to γ-carboxylated glutamyl residues.[34,35]

Note that non-bonded interactions are unrestrained throughout structure solution and refinement. As a result they can be considered as essentially experimental values. In this case, agreement between hydrogen bonding geometry in the structure reported here and in similar known structures is good with most reported values being well within the ranges suggested by the CSD. C8–H18A···O12A and C13–H20B···O11B are the only hydrogen bonds in the proposed scheme whose O···H distances do not lie well within the range of values taken from known structures and these interactions are therefore likely to be relatively weak.

The orientation of methyl groups (from the neutron refinement) is such that the methyl hydrogen atom furthest from O12 lies almost in the plane of the ring system, 13° or 11° away from the ring plane, in A or B respectively, see Fig. 6. The remaining two methyl hydrogens lie almost as far from the plane of the ring system as possible simultaneously, with one hydrogen atom ~50° and the other ~70° from the plane. This theme is common to a number of similar structures in the CSD,[36–38] with the methyl group ring substituent orientated such that the distance between methyl hydrogen atoms and an *ortho* oxygen atom is maximised, reducing the possibility of an intramolecular hydrogen bond between these atoms.

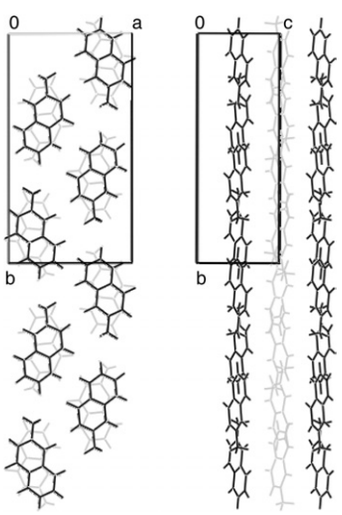

Fig. 7 Chains of symmetry equivalent molecules: dark grey molecules are type A and light grey molecules are type B. The views along *c* and *a* are shown.

3. Conclusions

The crystal structure of vitamin K_3 has been solved and separate restrained Rietveld refinements were carried out using powder X-ray and neutron diffraction data. The structural information in the neutron data is reduced by the low peak to background ratio; however in addition to providing

Table 4 Proposed hydrogen bonding scheme; numbers 1 to 8 correspond to Fig. 8

			C–H···O/°	O···H/Å	C–O···H/°	H···O···H/°	First order graph set descriptor
Refined Structure	C1–H14B···O11A	1	163.76	2.659	111.16	97.36	*D*
	C8–H18B···O11A	2	152.70	2.502	132.26		*D*
	C8–H18A···O12A	3	115.02	2.717	109.72	92.76	*C*(5)
	C3–H16B···O12A	4	138.28	2.509	149.53		*D*
	C13–H20B···O11B	5	131.51	2.737	124.86	90.83	$R_2^2(12)$
	C3–H16A···O11B	6	130.75	2.581	106.79		*D*
	C1–H14A···O12B	7	157.04	2.299	147.21	67.72	*D*
	C13–H21B···O12B	8	163.79	2.577	132.55		$R_2^2(10)$
CSD	Minimum		45.404	2.012	57.027	32.87	
	Maximum		178.79	2.720	177.17	167.35	
	Mean		146.95	2.5715	127.41	81.989	

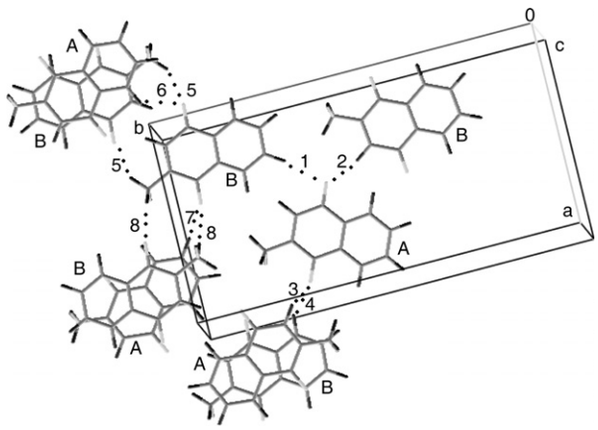

Fig. 8 The crystal structure refined using neutron diffraction data. The two central molecules represent the molecules in the asymmetric unit (A and B); surrounding C–H···O hydrogen bonds are indicated with dotted lines. Hydrogen bond numbers 1 to 8 correspond to those in Table 4.

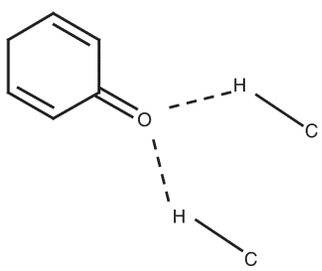

Fig. 9 Search fragment used to find comparable C–H···O interactions in the CSD.

confirmation of the crystal structure determined by X-ray diffraction, the neutron refinement provided additional insight in terms of the methyl group orientation. This allowed a detailed description of C–H···O hydrogen bonds, which have been elucidated by reference to similar known structures. The utility of powder neutron diffraction for refinement of organic molecules, as a complement to X-ray diffraction data, has been demonstrated in this study.

Acknowledgements

The authors thank Dr M. Brunelli for assistance with the BM16 experiment, Dr R. Ibberson for assistance with the HRPD experiment, EPSRC for provision of beam time and EPSRC and CCDC for funding.

References

1 S. F. Dyke, *The Chemistry of the Vitamins*, Interscience Publishers, London, 1965, ch. 15.
2 H. Rosenberg, *Chemistry and Physiology of the Vitamins*, Interscience Publishers Inc., New York, 1945, p. 481.
3 S. W. Ham, H. J. Park and D. H. Lim, *Bioorganic Chemistry*, 1997, **25**, 33.
4 W. Adam, W. A. Herrmann, J. Lin, C. T. Saha-Möller, R. W. Fischer and J. D. G. Correia, *Angew. Chem., Int. Ed. Engl.*, 1994, **33**, 2475.
5 K. D. M. Harris, M. Tremayne and B. M. Kariuki, *Angew. Chem., Int. Ed.*, 2001, **40**, 1626.
6 S. Kirkpatrick, C. D. Gelatt and M. P. Vecchi, *Science*, 1983, **220**, 671.
7 Cambridge Crystallographic Data Centre, *DASH–a program for structure solution from powder diffraction data*, CCDC, 12 Union Road, Cambridge, UK, 2001.
8 W. I. F. David, K. Shankland and N. Shankland, *Chem. Commun.*, 1998, **8**, 931.
9 S. Pagola, P. W. Stephens, D. S. Bohle, A. D. Kosar and S. K. Madsen, *Nature*, 2000, **404**, 307.
10 R. E. Dinnebier, M. Schweiger, B. Bildstein, K. Shankland, W. I. F. David, A. Jobst and S. van Smaalen, *J. Appl. Crystallogr.*, 2000, **33**, 1199.
11 S. G. Zhukov, V. V. Chernyshev, E. V. Babaev, E. J. Sonneveld and H. Schenk, *Z. Kristallogr.*, 2001, **216**, 5.
12 H. M. Rietveld, *Acta Crystallogr.*, 1967, **22**, 151.
13 H. M. Rietveld, *J. Appl. Crystallogr.*, 1969, **2**, 65.
14 R. B. Von Dreele, *J. Appl. Crystallogr.*, 1999, **32**, 1084.
15 M. Tremayne, B. M. Kariuki, K. D. M. Harris, K. Shankland and K. S. Knight, *J. Appl. Crystallogr.*, 1997, **30**, 968.
16 R. M. Ibberson, C. Morrison and M. Prager, *Chem. Commun.*, 2000, **7**, 539.
17 R. Taylor and O. Kennard, *J. Am. Chem. Soc.*, 1982, **104**, 5063.
18 F. H. Allen and O. Kennard, *Chem. Des. Autom. News*, 1993, **8**, 31.
19 R. M. Ibberson, W. I. F. David, and K. S. Knight, Rutherford Appleton Laboratory Report, RAL-92-031, 1992.
20 G. S. Pawley, *J. Appl. Crystallogr.*, 1981, **14**, 357.
21 H. Nowell, J. P. Attfield, J. C. Cole, P. J. Cox, K. Shankland, S. J. Maginn and W. D. S. Motherwell, *New. J. Chem.*, 2002, **26**, 469.
22 H. Nowell, J. P. Attfield and J. C. Cole, *Acta Crystallogr., Sect. B*, 2002, **58**, 835.
23 H. Nowell, J. P. Attfield, N. Shan, W. Jones and W. D. S. Motherwell, *Cryst. Eng.*, 2003, **6**, 1,57.
24 I. J. Bruno, J. C. Cole, P. R. Edgington, M. Kessler, C. F. Macrae, P. McCabe, J. Pearson and R. Taylor, *Acta Crystallogr., Sect. B*, 2002, **58**, 389.
25 P. Thompson, D. E. Cox and J. B. Hastings, *J. Appl. Crystallogr.*, 1987, **20**, 79.
26 L. W. Finger, D. E. Cox and A. P. Jephcoat, *J. Appl. Crystallogr.*, 1994, **27**, 892.
27 A. March, *Z. Kristallogr.*, 1932, **81**, 285.
28 W. A. Dollase, *J. Appl. Crystallogr.*, 1986, **19**, 267.
29 A. Boultif and D. Louër, *J. Appl. Crystallogr.*, 1991, **24**, 987.
30 R. Shirley, *The CRYSFIRE System for Automatic Powder Indexing: User's Manual*, The Lattice Press, 41 Guildford Park Avenue, Guildford, Surrey, UK GU2 7NL, 2000.
31 A. C. Larson and R. B. Von Dreele, *General Structure Analysis System (GSAS)*, Los Alamos National Laboratory Report LAUR 86-748, 1994.
32 M. C. Etter, *Acc. Chem. Res.*, 1990, **23**, 120.
33 M. C. Etter, J. C. MacDonald and J. Bernstein, *Acta Crystallogr., Sect. B*, 1990, **46**, 256.
34 B. N. Pudota, E. L. Hommema, K. W. Hallgren, B. A. McNally, S. Lee and K. L. Berkner, *J. Biol. Chem.*, 2001, **276**, 46878.
35 K. L. Berkner, *J. Nutr.*, 2000, **130**, 1877.
36 M. Soriano-Garcia, R. A. Toscano, E. Flores-Valverde, F. Montoya-Verga and I. Lopez-Celis, *Acta Crystallogr. Sect. C*, 1986, **42**, 327CSD refcode DIPVON.
37 V. Nair, A. U. Vinod, J. S. Nair, A. R. Sreekanth and N. P. Rath, *Tetrahedron Lett.*, 2000, **41**, 6675CSD refcode EBOHUY.
38 A. S. Batsanov, M. R. Bryce, S. R. Davies and J. A. K. Howard, *J. Mater Chem.*, 1994, **4**, 1719CSD refcode YISDIN.